BJR

https://doi.org/10.1259/bjr.20190558

Received: 24 June 2019 | Revised: 06 January 2020 | Accepted: 15 January 2020

Cite this article as:
Chen J, He B, Dong D, Liu P, Duan H, Li W, et al. Noninvasive CT radiomic model for preoperative prediction of lymph node metastasis in early cervical carcinoma. *Br J Radiol* 2020; **93**: 20190558.

FULL PAPER

Noninvasive CT radiomic model for preoperative prediction of lymph node metastasis in early cervical carcinoma

[1,2]JIAMING CHEN, [3,4,5]BINGXI HE, [3,5]DI DONG, [1,2]PING LIU, [1,2]HUI DUAN, [1,2]WEILI LI, [1,2]PENGFEI LI, [1,2]LU WANG, [1,2]HUIJIAN FAN, [3,5]SIWEN WANG, [3,5]LIWEN ZHANG, [3,5,6]JIE TIAN, [4,5]ZHIPEI HUANG and [1,2]CHUNLIN CHEN

[1]Department of Obstetrics and Gynecology, Nanfang Hospital, Southern Medical University, Guangzhou, China
[2]Digital Medical Laboratory of Department of Obstetrics and Gynecology, Nanfang Hospital, Southern Medical University, Guangzhou, China
[3]CAS Key Laboratory of Molecular Imaging, Institute of Automation, Chinese Academy of Sciences, Beijing, China
[4]School of Electronic, Electrical and Communication Engineering, University of Chinese Academy of Sciences, Beijing, China
[5]University of Chinese Academy of Sciences, Beijing, China
[6]Beijing Advanced Innovation Center for Big Data-Based Precision Medicine, Beihang University, Beijing, China

Address correspondence to:
Jie Tian
E-mail: *jie.tian@ia.ac.cn*
Zhipei Huang
E-mail: *zhphuang@ucas.ac.cn*
Chunlin Chen
E-mail: *ccl1@smu.edu.cn*

The authors Jiaming Chen, Bingxi He and Di Dong contributed equally to the work.

Objective: To build and validate a CT radiomic model for pre-operatively predicting lymph node metastasis in early cervical carcinoma.
Methods and materials: A data set of 150 patients with Stage IB1 to IIA2 cervical carcinoma was retrospectively collected from the Nanfang hospital and separated into a training cohort (n = 104) and test cohort (n = 46). A total of 348 radiomic features were extracted from the delay phase of CT images. Mann–Whitney U test, recursive feature elimination, and backward elimination were used to select key radiomic features. Ridge logistics regression was used to build a radiomic model for prediction of lymph node metastasis (LNM) status by combining radiomic and clinical features. The area under the receiver operating characteristic curve (AUC) and κ test were applied to verify the model.
Results: Two radiomic features from delay phase CT images and one clinical feature were associated with LNM status: log-sigma-2-0 mm-3D_glcm_Idn (p = 0.01937), wavelet-HL_firstorder_Median (p = 0.03592), and Stage IB (p = 0.03608). Radiomic model was built consisting of the three features, and the AUCs were 0.80 (95% confidence interval: 0.70 ~ 0.90) and 0.75 (95% confidence intervall: 0.53 ~ 0.93) in training and test cohorts, respectively. The κ coefficient was 0.84, showing excellent consistency.
Conclusion: A non-invasive radiomic model, combining two radiomic features and a International Federation of Gynecology and Obstetrics stage, was built for prediction of LNM status in early cervical carcinoma. This model could serve as a pre-operative tool.
Advances in knowledge: A noninvasive CT radiomic model, combining two radiomic features and the International Federation of Gynecology and Obstetrics stage, was built for prediction of LNM status in early cervical carcinoma.

INTRODUCTION

Cervical carcinoma is a common malignant tumor, with an annual worldwide incidence of 500,000, more than 80% of which are in developing countries.[1] In China, the incidence and mortality of cervical carcinoma are 98,900 and 30,500 in 2015, respectively.[2]

Surgery and adjuvant therapy are the main therapy options for cervical carcinoma. Lymph node metastasis (LNM) is an independent risk factor for the outcome of cervical carcinoma, and pelvic lymphadenectomy (PLD) is routinely recommended during surgery, which is required for cervical

carcinoma with International Federation of Gynecology and Obstetrics (FIGO) Stage IA1 with LVSI and Stage IA2 to IIA2.[3]

Previous studies reported that no more than 30% of early cervical carcinoma patients had LNM,[4–7] which suggests that 70% of patients underwent unnecessary PLD, and some even underwent unnecessary lymph node (LN) radiotherapy. Such overtreatment is caused by inaccurate LNM staging before surgery. The gold-standard for LNM staging is post-operative histology. However, a surgeon needs to dissect important vessels, which is associated with high difficulty, high risk, and a series of intraoperative and post-operative complications.[8–11] Pre-operative diagnosis of LNM is mainly dependent on CT and MRI based on the morphology of LN, which suffers from great subjectivity.[12–14] Therefore, new methods for accurate diagnosis of LNM before surgery are needed to help doctors establish personalized PLD schedules.

Recently, radiomics has been proposed to extract rich information by quantitative and high throughput analysis of conventional medical images.[15,16] It has been used to estimate LNM status by extracting quantitative characteristics from CT images related to bladder, colorectal, breast, thyroid, esophageal, and lung adenocarcinoma, and the radiomics nomogram showed good predictive performance.[17–23] Therefore, the intention of this study was to assess the LNM status in individuals affected by cervical carcinoma by using a CT radiomics method. To accomplish this, we developed a radiomic model to obtain predictions of the LNM status pre-operatively.

METHODS AND MATERIALS

Patients

This was a retrospective study, and requirement for patients' informed consent was waived by the institutional review board of Nanfang hospital. We reviewed records from between 2008 and 2018. Considering the longest time required for the effects of the drugs to be apparent in CT images, the experiments were performed first on patients with a delay phase. A total of 172 cervical carcinoma cases with a FIGO stage from IB1 to IIA2 were included in accordance with the following criteria: (1) post-operative histology confirmed cervical carcinoma and LN status; (2) no pre-operative adjuvant therapy; (3) pre-operative CT images (thickness of 1.0 or 1.5 mm) and available clinical data; (4) no other malignant tumors; (5) patients with complete delay phase CT images. 22 patients were excluded for the following criteria: (1) maximum diameter of the tumor was less than 20 pixels; (2) metal artifacts exist in images. Finally, 150 patients with delay phase CT scans were enrolled and sorted by CT acquired time; the first 70% of the patients were used as the training cohort (n = 104, containing 21 LNM patients and 83 non-LNM patients), the remainder as the test cohort (n = 46, containing 10 LNM patients and 36 non-LNM patients).

Clinical and pathologic features

Clinical, imaging, and pathological information were collected from the hospital system (DHC-EMR; Table 1). Clinical features included age, menarche time, pregnancy and parturition numbers, FIGO stage, and histological type of tumor. Imaging features included the status of corpus uteri, vagina, and LN on CT reports. Pathological information included the status of LNM after surgery.

CT image acquisition

All patients were scanned by the SIEMENS Definition Double Source CT (SOMA-TOM Definition, Siemens Ltd, Germany). Scanning range was from the upper margin of the kidney to 2 cm off the lower edge of the pubic symphysis. We used a double tube high pressure syringe at a speed of 3.5 $ml\,s^{-1}$ to engage patients with a right cubital vein injection of 75 ml non-ionic iodine contrast agent Ultravist (370 $mgL\,ml^{-1}$, Schering Pharmaceutical Co. Ltd. Guangzhou Germany), followed with 30 ml normal saline. At the same time, aortic bifurcation 2.0 cm above the region of interest (ROI) was performed using contrast tracer method (BOLUS TRACKING) dynamic monitoring of CT; an automatic trigger scan ROI was setup when the CT value reached 120 HU. After 35 s priming delayed venous phase scanning and 120 s trigger delayed phase scanning, venous phase and delayed phase image capture were performed, respectively. All images were derived in the DICOM3.0 format.

Tumor segmentation

ROI segmentation was indispensable for feature extraction. One gynecologist with 5 years of experience (Observer 1) manually delineated two-dimensional ROI (the largest area of the primary tumor) on all original images of plain scan, arterial phase, venous phase, and delayed phase, using the ITK-SNAP open-source software (www.itk-snap.org). Another gynecologist with 10 years of experience (Observer 2) examined all the segmentations. Observer 2 selected 30 cases randomly and re-delineated the ROIs to test the interobserver error.

Radiomic feature extraction

We obtained a series of CT scans with mean values of 0 and variance of 1 by using z-score method in the training cohort, and then re-sampled these CT scans to ensure that each scan had the same layer to layer and voxel to voxel spacing.

Then, two-dimensional radiomic features were extracted from the ROIs. Image transformation used two types of filters (Figure 1): (I) Wavelet filter, and (II) Laplacian of Gaussian (LOG) filter. The radiomic features were divided into three groups: (I) first-order statistical features, (II) morphological features, and (III) texture features. The explanations of radiomics features and image filters are detailed in Supplementary Material 1.

Statistical analysis

For the LNM class, we used label encoding to represent discrete properties in terms of numbers, and binarized these numbers by one-hot encoding. Apart from making features sparse, one-hot encoding can also add the number of features. The output of the model is the probability of LNM.

The Mann–Whitney U test was used to examine the significance of radiomic features (p-value < 0.05 was considered significant). To eliminate redundant features with collinearity, we carried out recursive feature elimination (RFE) with cross-validation. RFE

Table 1. Clinical features of patients

	Training cohort		Test cohort		
Feature	**No.**	**Mean ± SD**	**No.**	**Mean ± SD**	***p***
Age		47.87 ± 10.61		45.80 ± 13.72	0.499
FIGO stage					**<0.001***
IB	77		38		
IIA	27		8		
Pregnancy		3.77 ± 2.00		3.76 ± 1.92	0.1155
Histologic type					0.3996
Squamous carcinoma	82		38		
Non-squamous carcinoma	21		6		
Parturition		2.77 ± 1.47		2.43 ± 1.47	0.1319
Menarche time		14.26 ± 2.76		13.70 ± 3.78	0.0537
CT-reported LN status					0.1445
Negative	84		39		
Positive	15		5		
CT-reported vagina status					0.1464
Negative	96		42		
Positive	3		2		
CT-reported uterus status					0.4678
Negative	97		37		
Positive	2		7		

FIGO, International Federation of Gynecology and Obstetrics; LN, lymph node; SD, standard deviation.
Note. p value was calculated from univariable analysis between each of the clinical features and LN status. *p-value < 0.05.

Figure 1. Inclusion and exclusion criteria.

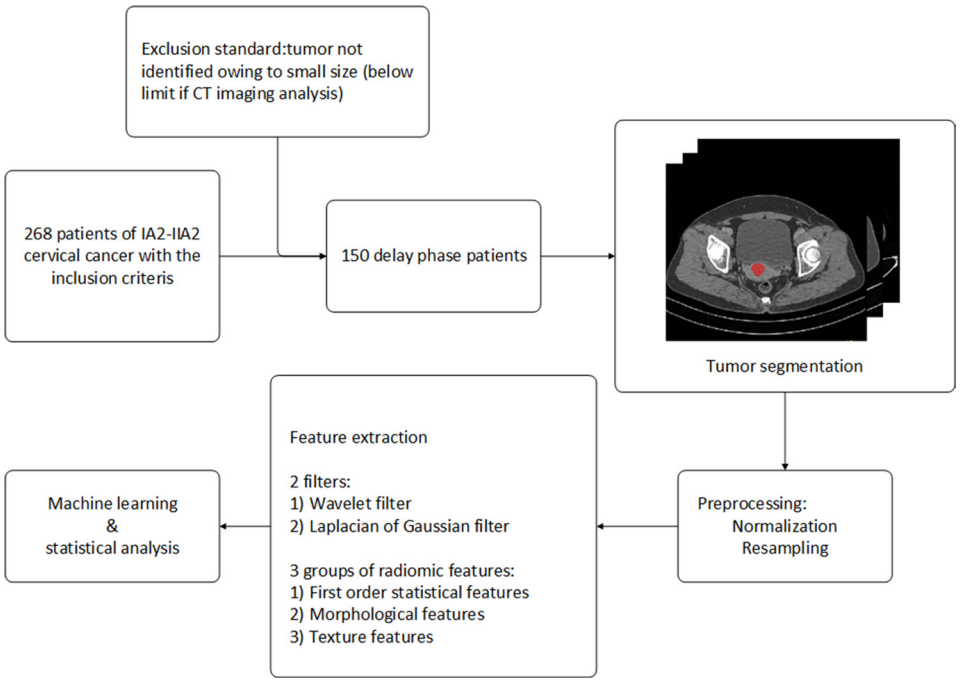

Figure 2. Flow chart of statistical analysis.

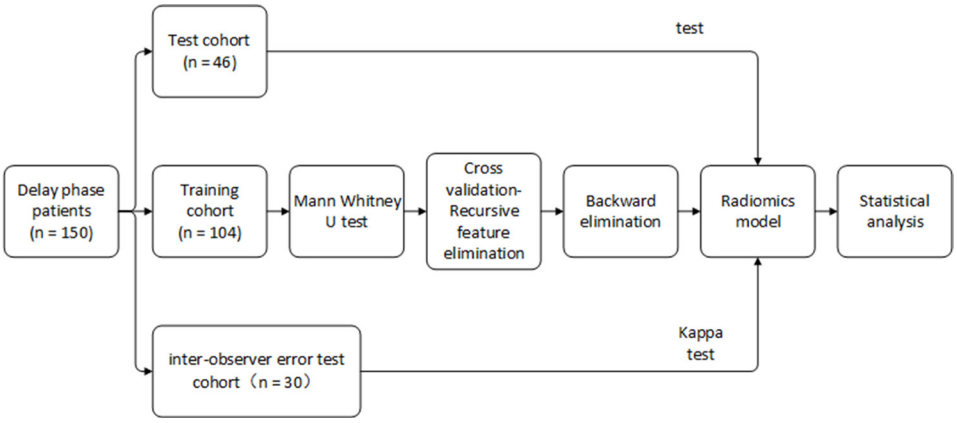

is a greedy algorithm for finding a preferable feature subset; the underlying RFE model used here was ridge logistic regression. We choose backward elimination to identify optimum feature combination by adding all variables to the regression equation at one time and then sequentially removing single variable that did not significantly affect the regression equation until all variables were significant. What needs to be added is that the multivariate p-value < 0.05 indicates that the effect on the regression equation is significant.

Logistic regression with L2-norm was used to construct the radiomic model. Owing to the unbalanced samples, class weights were adjusted. Model performance was assessed by the receiver operating characteristic (ROC) curve and the area under the curve (AUC). At the same time, we also used a calibration curve to evaluate the model. Decision curve analysis helps choose the model that predicts the greatest net benefit. The abscissa indicates the threshold probability and the ordinate indicates the net benefit. The higher the decision curve, the better the model's net income. Furthermore, we performed an interobserver error test on segmentation results from the 30 selected patients and calculated the κ coefficient between the two results (κ coefficient >0.6 indicates a feature with high consistency).

We used Python (URL: https://www.python.org/, v. 3.6.5) to extract features and perform statistical analysis (Figure 2). The "pyradiomics" package was used to extract radiomics features. The "scikit-learn" package was applied for RFE, cross-validation, ridge logistic regression, and model evaluation.

RESULTS

Clinical features and radiomic features

This study contained 150 patients (104 in the training cohort and 46 in the test cohort). The mean age were 47.87 ± 10.61 and 45.80 ± 13.72 in the training cohort and test cohort, respectively. 77 patients of IB stage and 27 patients of IIA stage were in the training cohort, and 38 patients of IB stage and 8 patients of IIA stage were in the test cohort. Squamous carcinoma and non-squamous carcinoma in the training and test cohort were 82 and 21, and 38 and 6, respectively. 15 and 5 patients were reported LNM by CT in the training and test cohort. We extracted 348 radiomic features from the tumor ROI, including 108 first-order statistical features, 12 morphological features, and 232 texture features.

As shown in Figure 3, the performance (accuracy) of the model was best when the number of features was 10. In light of the backward elimination results, three features were selected for modeling[1]: log-sigma-2–0 mm-3D_glcm_Idn (Inverse Difference Normalized), representing the local homogeneity of the CT after using the LOG filter[2]; wavelet-hl_firstorder_median, representing the median gray level intensity in the ROI after using the wavelet filter (HL)[3]; Stage IB, representing that the patient's FIGO stage was IB. The p-values in multivariate analysis were less than 0.0001. The distribution of these features is shown in Figure 3.

Apparent performance of the radiomics model

We used the three selected features to build a radiomics model, which was then applied in the test cohort for testing. The ROC curves of the radiomic model in the training and test cohorts are shown in Figure 4. The AUCs of the radiomic model in the training and test cohorts were 0.80 [95% confidence interval (CI): 0.70–0.90] and 0.75 (95%CI: 0.53–0.93), respectively, indicating that the model was a good predictor of LNM. In addition, we removed clinical features and only used radiomic features to build a model [AUC: 0.73 (95%CI: 0.60–0.85) Figure 4], and found that the addition of clinical features could significantly improve the performance of the model. The decision curve of the radiomic model is shown in Figure 4. We found that when the threshold probability was larger than 5%, the radiomic model was more effective than treat-all and treat-none schemes.

Validation of the radiomics model

The result of the κ test between the two segmentations (*i.e.* those performed by the two observers) was 0.84, indicating excellent consistency of the features.

We further investigated the phases by supplementing 149 patients with arterial phase and 146 patients with venous phase to implement the prediction of LNM. We found that there were no significant radiomics features for arterial phase patients and a non-significant prediction result for venous phase patients.

Figure 3. (a) showed the model performance evaluated through the numbers of features as a function of the cross-validation feature recursive elimination algorithm. (b–e) Were statistical charts for the optimal subset of features. (b, c) Were violin-plots of radiomic features in the training cohort and test cohort, respectively. (d, e) Showed count-plots of clinical features in the training cohort and test cohort, respectively.

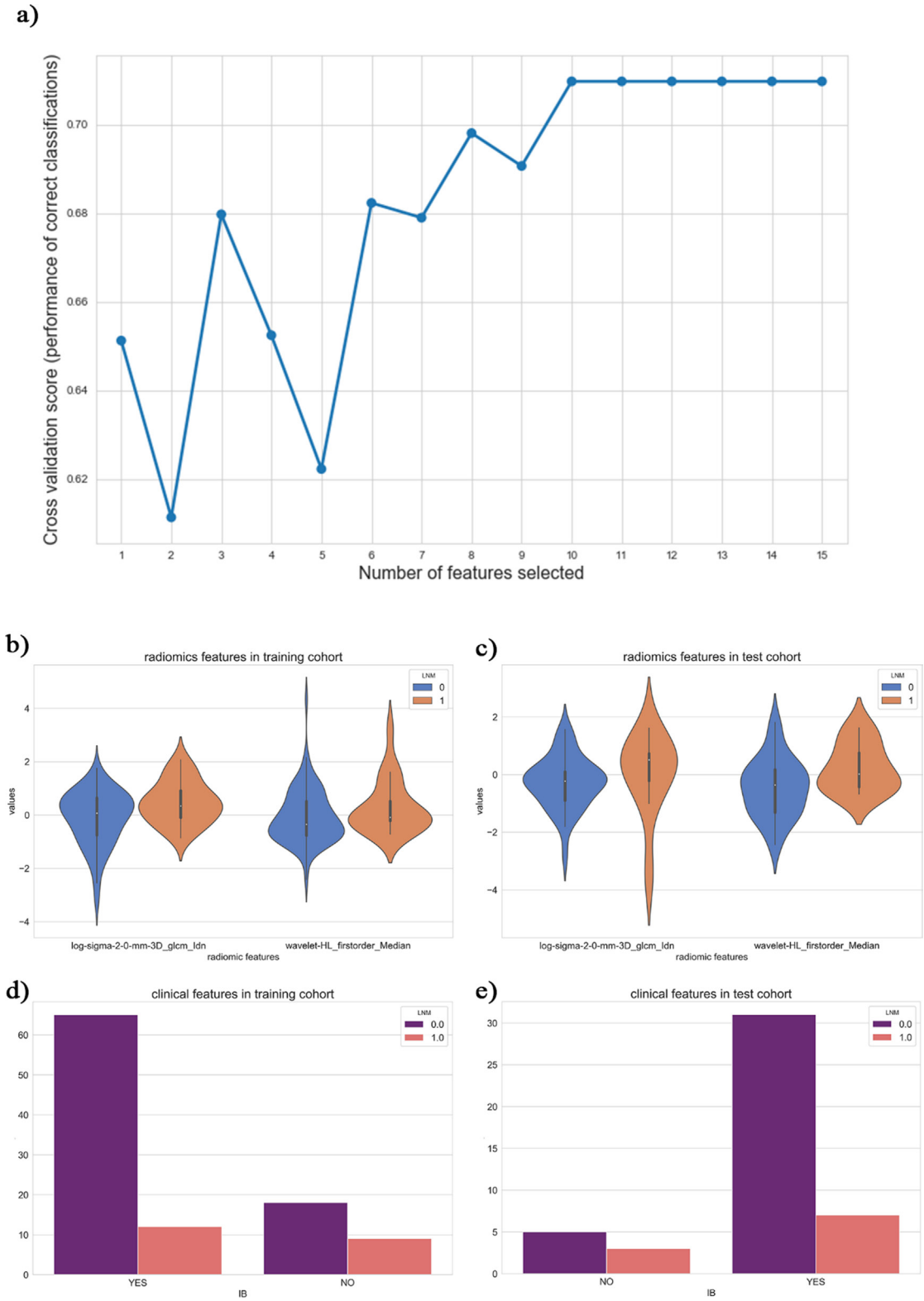

Figure 4. (a) Was the ROC curve of radiomic models for the training cohort (red, green, and yellow lines) and test cohort (blue line). (b) was the decision curve for the radiomics model (red line), clinical model (green line), radiomics model only using radiomics features (yellow line), treat-all (thin black line), and treat-none (thick black line) schemes. The thin black line represented the assumption that all patients have LNM; the thick black thick represented the assumption that none of the patients have LNM. LNM, lymph node metastasis; ROC, receiver operating characteristic

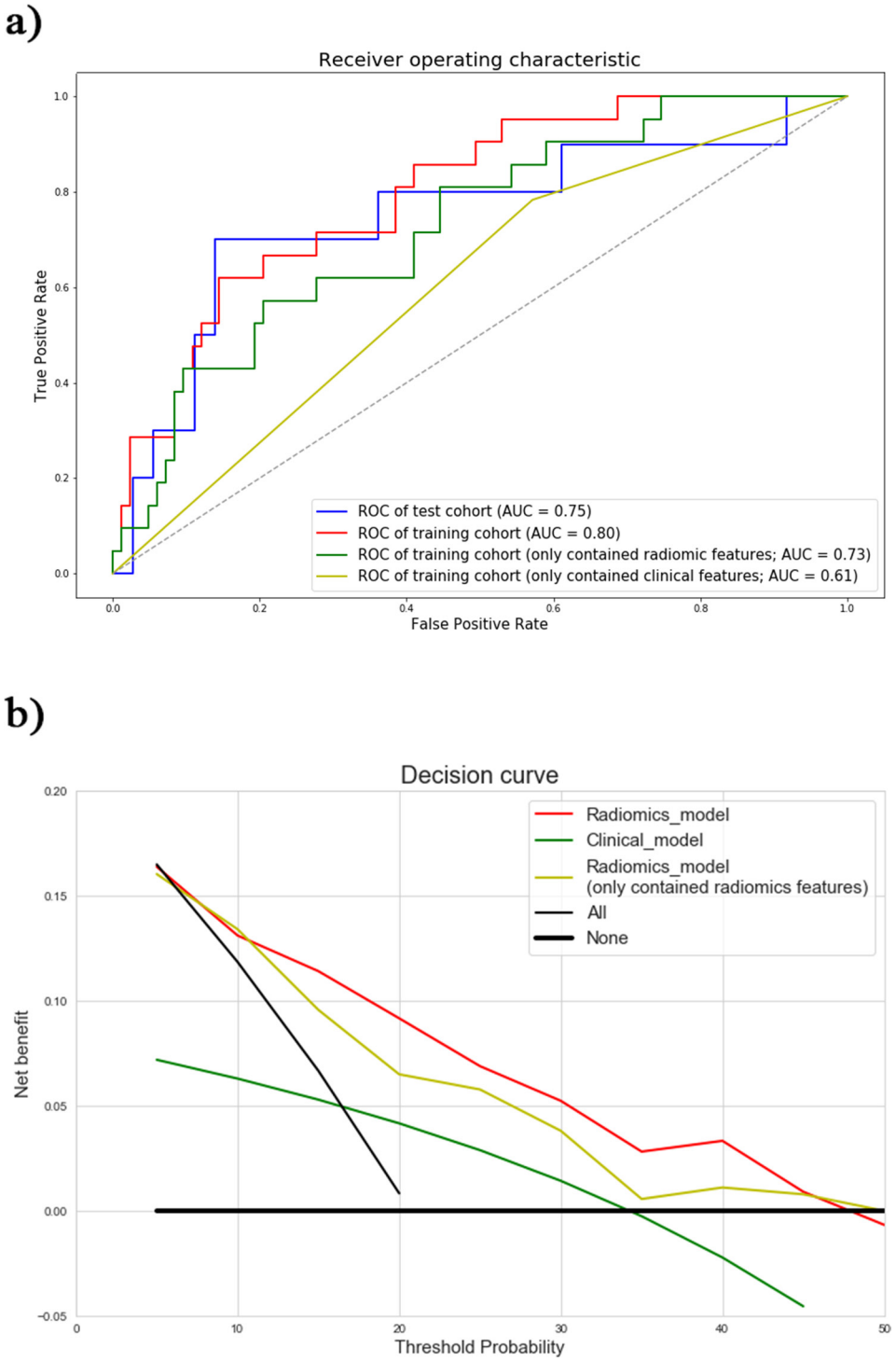

DISCUSSION AND CONCLUSION

We developed and validated a CT radiomic model for preoperative prediction of LNM in early cervical carcinoma. By the validation in the test set, we found that the radiomic model had good predictive capacity. This study tested radiomic and clinical features to establish the model, and three features were singled out: (1) log-sigma-2–0 mm-3D_glcm_Idn (Inverse Difference Normalized); (2) wavelet-hl_firstorder_median ; (3) Stage IB.

The main pre-operative techniques for predicting LNM are LN ultrasonography, CT, MRI, positron emission tomography-CT (PET-CT), and needle aspiration biopsy of LN. Ultrasonography is only suitable for superficial LN, but is unsatisfactory for deep LN such as pelvic lymph nodes. CT and MRI are the most widely used imaging examinations for LN diagnosis. Criteria for determining LNM are based on morphology (*e.g.* shortest diameter more than 1 cm, uneven density of LN, central necrosis, coarse envelope, or shape of the circle from an ellipse). The sensitivity and specificity of CT and MRI in the diagnosis of LN are 64–72%, and 93–93%, respectively.[12] These two methods have certain subjectivities, making it difficult to distinguish metastatic LN and inflammatory LN.[12–14] Consequently, the evaluating performance is poor, and the diameters of metastatic LN with more than 40% are less than 1 cm.[24,25]

Many hospitals lack PET-CT equipment, and the cost of inspection is very high; therefore, this approach is not widely used at present. Some researchers have suggested that the value of FDG-PET for LNM diagnosis is not as good as that using MRI, where sensitivity and specificity in detecting pelvic LN were 67 and 84% with MRI, and 33 and 92% with FDG-PET in their study.[14,26]

The 2018 National Comprehensive Cancer Network clinical practice guidelines no longer recommend LN needle aspiration biopsy.[3] Errors in pre-operative molecular detection of solid tumors are spatially and temporally heterogeneous, but relatively non-invasive medical imaging examination could provide more comprehensive information.[27]

The limitations of our study were as follows. First, all data were from a single center. Multicenter external validation with a larger simple size is needed to improve the predictive capacity of the model for clinical application. Second, we only identified the largest area of the primary tumor. Therefore, this study lacked three-dimensional radiomics analysis. Third, only CT data were used for radiomics analysis; it may be better to combine pre-operative biopsy pathological images or MRI data to construct the model and that will be our future direction of work.

In conclusion, this radiomic model, which combined two radiomic features and FIGO stage, is a non-invasive tool that shows good performance. It could be potentially and conveniently used for assessing LNM status individually before surgery in early cervical carcinoma patients. Furthermore, the use of this model could avoid unnecessary PLD, which would reduce treatment risks and the financial burden of these patients.

ACKNOWLEDGMENT

We would like to express our gratitude for financial support from the National Key R&D Program of China (2017YFC1308700, 2017YFA0205200, 2017YFC1309100, 2017YFC1308701, 2016YFC0103803, 2017YFA0700401), the National Natural Science Foundation of China (81571422, 81370736, 81771924, 81501616, 81227901, 81671851, 81527805, 61671449, 61622117), the National Science and Technology Support Program of China (2014BAI05B03), the National Natural Science Fund of Guangdong (2015A030311024), the Science and Technology Plan of Guangzhou (158100075), the Beijing Municipal Science and Technology Commission (Z171100000117023, Z161100002616022), the Instrument Developing Project of the Chinese Academy of Sciences (YZ201502), and the Youth Innovation Promotion Association CAS (2017175).

REFERENCES

1. Tsu V, Jerónimo J. Saving the world's women from cervical cancer. *N Engl J Med* 2016; **374**: 2509–11. doi: https://doi.org/10.1056/NEJMp1604113
2. Chen W, Zheng R, Baade PD, Zhang S, Zeng H, Bray F, et al. Cancer statistics in China, 2015. *CA Cancer J Clin* 2016; **66**: 115–32. doi: https://doi.org/10.3322/caac.21338
3. Koh W-J, Abu-Rustum NR, Bean S, Bradley K, Campos SM, Cho KR, et al. Uterine neoplasms, version 1.2018, NCCN clinical practice guidelines in oncology. *J Natl Compr Canc Netw* 2018; **16**: 170–99. doi: https://doi.org/10.6004/jnccn.2018.0006
4. Sakuragi N, Satoh C, Takeda N, Hareyama H, Takeda M, Yamamoto R, et al. Incidence and distribution pattern of pelvic and paraaortic lymph node metastasis in patients with stages Ib, IIA, and IIB cervical carcinoma treated with radical hysterectomy. *Cancer* 1999; **85**: 1547–54. doi: https://doi.org/10.1002/(SICI)1097-0142(19990401)85:7<1547::AID-CNCR16>3.0.CO;2-2
5. Martínez A, Mery E, Filleron T, Boileau L, Ferron G, Querleu D. Accuracy of intraoperative pathological examination of SLN in cervical cancer. *Gynecol Oncol* 2013; **130**: 525–9. doi: https://doi.org/10.1016/j.ygyno.2013.01.023
6. Ditto A, Martinelli F, Lo Vullo S, Reato C, Solima E, Carcangiu M, et al. The role of lymphadenectomy in cervical cancer patients: the significance of the number and the status of lymph nodes removed in 526 cases treated in a single institution. *Ann Surg Oncol* 2013; **20**: 3948–54. doi: https://doi.org/10.1245/s10434-013-3067-6
7. Du R, Li L, Ma S, Tan X, Zhong S, Wu M. Lymph nodes metastasis in cervical cancer: incidences, risk factors, consequences and imaging evaluations. *Asia Pac J Clin Oncol* 2018;.
8. Querleu D, Leblanc E, Cartron G, Narducci F, Ferron G, Martel P. Audit of preoperative and early complications of laparoscopic lymph node dissection in 1000 gynecologic cancer patients. *Am J Obstet Gynecol* 2006; **195**: 1287–92. doi: https://doi.org/10.1016/j.ajog.2006.03.043
9. Achouri A, Huchon C, Bats AS, Bensaid C, Nos C, Lécuru F. Complications of lymphadenectomy for gynecologic cancer. *Eur J Surg Oncol* 2013; **39**: 81–6. doi: https://doi.org/10.1016/j.ejso.2012.10.011
10. Musch M, Klevecka V, Roggenbuck U, Kroepfl D. Complications of pelvic lymphadenectomy in 1,380 patients undergoing radical retropubic prostatectomy between 1993 and 2006. *J Urol* 2008; **179**: 923–9. doi: https://doi.org/10.1016/j.juro.2007.10.072
11. Tanaka T, Ohki N, Kojima A, Maeno Y, Miyahara Y, Sudo T, et al. Radiotherapy negates the effect of retroperitoneal

nonclosure for prevention of lymphedema of the legs following pelvic lymphadenectomy for gynecological malignancies: an analysis from a questionnaire survey. *Int J Gynecol Cancer* 2007; **17**: 460–4. doi: https://doi.org/10.1111/j.1525-1438.2007.00869.x

12. Kasuya G, Toita T, Furutani K, Kodaira T, Ohno T, Kaneyasu Y, et al. Distribution patterns of metastatic pelvic lymph nodes assessed by CT/MRI in patients with uterine cervical cancer. *Radiat Oncol* 2013; **8**: 139. doi: https://doi.org/10.1186/1748-717X-8-139
13. Pelikan HMP, Trum JW, Bakers FCH, Beets-Tan RGH, Smits LJM, Kruitwagen RFPM. Diagnostic accuracy of preoperative tests for lymph node status in endometrial cancer: a systematic review. *Cancer Imaging* 2013; **13**: 314–22. doi: https://doi.org/10.1102/1470-7330.2013.0032
14. Park J-Y, Lee JJ, Choi HJ, Song IH, Sung CO, Kim HO, et al. The value of preoperative positron emission tomography/computed tomography in node-negative endometrial cancer on magnetic resonance imaging. *Ann Surg Oncol* 2017; **24**: 2303–10. doi: https://doi.org/10.1245/s10434-017-5901-8
15. Lambin P, Leijenaar RTH, Deist TM, Peerlings J, de Jong EEC, van Timmeren J, et al. Radiomics: the bridge between medical imaging and personalized medicine. *Nat Rev Clin Oncol* 2017; **14**: 749–62. doi: https://doi.org/10.1038/nrclinonc.2017.141
16. Wang S, Shi J, Ye Z, Dong D, Yu D, Zhou M, et al. Predicting EGFR mutation status in lung adenocarcinoma on computed tomography image using deep learning. *Eur Respir J* 2019; **53**: 1800986. doi: https://doi.org/10.1183/13993003.00986-2018
17. Wu S, Zheng J, Li Y, Yu H, Shi S, Xie W, et al. A Radiomics nomogram for the preoperative prediction of lymph node metastasis in bladder cancer. *Clin Cancer Res* 2017; **23**: 6904–11. doi: https://doi.org/10.1158/1078-0432.CCR-17-1510
18. Huang Y-Q, Liang C-H, He L, Tian J, Liang C-S, Chen X, et al. Development and validation of a Radiomics nomogram for preoperative prediction of lymph node metastasis in colorectal cancer. *J Clin Oncol* 2016; **34**: 2157–64. doi: https://doi.org/10.1200/JCO.2015.65.9128
19. Zhong Y, Yuan M, Zhang T, Zhang Y-D, Li H, Yu T-F. Radiomics approach to prediction of occult mediastinal lymph node metastasis of lung adenocarcinoma. *AJR Am J Roentgenol* 2018; **211**: 109–13. doi: https://doi.org/10.2214/AJR.17.19074
20. Shen C, Liu Z, Wang Z, Guo J, Zhang H, Wang Y, et al. Building CT Radiomics based nomogram for preoperative esophageal cancer patients lymph node metastasis prediction. *Transl Oncol* 2018; **11**: 815–24. doi: https://doi.org/10.1016/j.tranon.2018.04.005
21. Dong D, Tang L, Li Z-Y, Fang M-J, Gao J-B, Shan X-H, et al. Development and validation of an individualized nomogram to identify occult peritoneal metastasis in patients with advanced gastric cancer. *Ann Oncol* 2019; **30**: 431–8. doi: https://doi.org/10.1093/annonc/mdz001
22. Dong Y, Feng Q, Yang W, Lu Z, Deng C, Zhang L, et al. Preoperative prediction of sentinel lymph node metastasis in breast cancer based on radiomics of T2-weighted fat-suppression and diffusion-weighted MRI. *Eur Radiol* 2018; **28**: 582–91. doi: https://doi.org/10.1007/s00330-017-5005-7
23. Liu T, Ge X, Yu J, Guo Y, Wang Y, Wang W, et al. Comparison of the application of B-mode and strain elastography ultrasound in the estimation of lymph node metastasis of papillary thyroid carcinoma based on a radiomics approach. *Int J Comput Assist Radiol Surg* 2018; **13**: 1617–27. doi: https://doi.org/10.1007/s11548-018-1796-5
24. Aoki T, Tomoda Y, Watanabe H, Nakata H, Kasai T, Hashimoto H, et al. Peripheral lung adenocarcinoma: correlation of thin-section CT findings with histologic prognostic factors and survival. *Radiology* 2001; **220**: 803–9. doi: https://doi.org/10.1148/radiol.2203001701
25. Valls C, Andía E, Sanchez A, Fabregat J, Pozuelo O, Quintero JC, et al. Dual-Phase helical CT of pancreatic adenocarcinoma: assessment of resectability before surgery. *AJR Am J Roentgenol* 2002; **178**: 821–6. doi: https://doi.org/10.2214/ajr.178.4.1780821
26. Monteil J, Maubon A, Leobon S, Roux S, Marin B, Renaudie J, et al. Lymph node assessment with (18)F-FDG-PET and MRI in uterine cervical cancer. *Anticancer Res* 2011; **31**: 3865–71.
27. Lambin P, Rios-Velazquez E, Leijenaar R, Carvalho S, van Stiphout RGPM, Granton P, et al. Radiomics: extracting more information from medical images using advanced feature analysis. *Eur J Cancer* 2012; **48**: 441–6. doi: https://doi.org/10.1016/j.ejca.2011.11.036